Scientific Research Publishing

Open Journal of Stomatology, 2025, 15(11), 315-333
https://www.scirp.org/journal/ojst
ISSN Online: 2160-8717
ISSN Print: 2160-8709

Minimizing Vascular Injury in Sinus Floor Elevation: A Cone Beam Computed Tomography Study of the Posterior Superior Alveolar Artery

Krishan Sarna[1*], Fawzia Butt[2], Joseph Gakonyo[3], Jimmy Gakure Njoroge[2], Beda Olabu[4]

[1]Unit of Oral and Maxillofacial Surgery, Oral Pathology and Oral Medicine, Division of Oral and Maxillofacial Surgery, Department of Dental Sciences, University of Nairobi, Nairobi, Kenya
[2]Department of Human Anatomy and Medical Physiology, University of Nairobi, Nairobi, Kenya
[3]Private practice in Oral implantology, Summit Dental Care, Nairobi, Kenya
[4]Unit of Human Anatomy, Department of Biomedical Sciences, The Aga Khan University, Nairobi, Kenya
Email: *krishnasarna@gmail.com, Fawziamaxfax@gmail.com, Josegaks@gmail.com, jimmygakure02@gmail.com, Otienobeda@gmail.com

How to cite this paper: Sarna, K., Butt, F., Gakonyo, J., Njoroge, J.G. and Olabu, B. (2025) Minimizing Vascular Injury in Sinus Floor Elevation: A Cone Beam Computed Tomography Study of the Posterior Superior Alveolar Artery. *Open Journal of Stomatology*, **15**, 315-333.
https://doi.org/10.4236/ojst.2025.1511029

Received: October 29, 2025
Accepted: November 23, 2025
Published: November 26, 2025

Abstract

Objective: The intimacy of the posterior superior alveolar artery (PSAA) with the lateral sinus wall makes it significant during sinus floor elevation for implant placement in the posterior maxilla. The objective of this study was to analyze crucial anatomical variations using cone beam computed tomography (CBCT). **Materials and methods:** 356 maxillary sinuses (178 CBCT scans—95 males and 83 females) were analyzed for the rate of detection of the PSAA, location relative to the lateral wall of the maxillary sinus, and distance of the PSAA to the sinus floor. The prevalence of any additional branches of the PSAA was recorded. **Results:** The PSAA was identified bilaterally in 150 cases (84.3%), unilaterally in 2 cases (1.12%,) and was undetectable in 26 cases (14.6%). The intraosseous course was most frequent in the molar region and a near-equal distribution between intraosseous and beneath the sinus membrane in the premolar region. The mean diameter of the PSAA was 1.67 ± 0.34 mm. The distance to the maxillary sinus floor measured 13.46 ± 4.24 mm, whereas the distance to the alveolar crest was 22.53 ± 2.32 mm. Two branches of the PSAA were observed in 27.34% (n = 82) of the cases. On average, the second branch was 12.34 ± 3.65 mm from the maxillary sinus floor and 21.89 ± 3.51 mm from the alveolar crest. **Conclusion:** Antrostomy preparation should be performed as mesial and as low as possible with a slight inferior curve around the area of the second premolar and first molar.

Keywords

Posterior Superior Alveolar Artery, Maxillary Sinus, Dental Implants, Lateral Sinus Floor Elevation, Surgical Complications

1. Introduction

Dental implant-supported prostheses are used worldwide due to their high survival and success rates [1]. One of the most fundamental requirements in implant placement is the availability of adequate bone volume to attain adequate primary stability. However, the atrophic posterior maxilla often presents a challenge due to insufficient vertical bone height. This deficiency arises from alveolar ridge resorption and maxillary sinus pneumatization, making implant placement surgically demanding [2]. To overcome this limitation, sinus floor elevation (SFE) is commonly performed to increase vertical bone volume, allowing for implant placement and grafting with biomaterials [3]. When the remaining subantral bone height is less than 4mm, the lateral window approach is a commonly used technique in which a bony window is created to access the antral cavity [4].

During SFE, intraoperative complications such as perforation of the Schneiderian membrane and hemorrhagic episodes due to vascular injury do sometimes occur [5]. Specifically, the posterior superior alveolar artery (PSAA), a critical structure closely related to the lateral sinus wall, can be lacerated or transected by rotary instruments during lateral window preparation. Although the haemorrhage from this vessel may not be life-threatening, it can cause visual obstruction of the surgical field, thus making membrane perforation more likely [6].

The PSAA originates from the maxillary artery's third (pterygopalatine) segment. It branches off within the pterygopalatine fossa, either as a single vessel or in conjunction with the infraorbital artery, and exits through the pterygomaxillary fissure. It then travels forward and is intimately related to the lateral wall of the maxillary sinus [7]. Here, it provides arterial supply to the maxillary sinus and the maxillary premolar and molar teeth. Although the general anatomy is reasonably well documented, the vessel exhibits substantial variations in its diameter and course [8]. Such variations put the vessel at risk of iatrogenic injury with consequent haemorrhage not only during placement of dental implants in the posterior maxilla but also during open sinus lifts, Caldwell-Luc surgeries, Le Fort 1 osteotomies, and osteosynthesis of maxillary fractures [9].

Literature on the subject reveals that the PSAA is affected by factors such as gender, geographical location, and ethnicity of the subjects being studied [8]. Notably, some of the most intriguing variations involve the artery's relationship with the lateral wall of the maxillary sinus. The PSAA may be embedded in the lateral bony wall of the sinus, situated beneath the sinus membrane within the sinus, or on the external cortex of the lateral wall. Furthermore, the distance between the artery and key landmarks, such as the maxillary sinus floor and the alveolar crest,

is highly variable, which can have significant clinical implications [9]-[12]. In pursuit of optimal imaging modalities to evaluate PSAA variations, cone beam computed tomography (CBCT) has emerged as a superior choice, offering distinct advantages such as a reduction in patient radiation exposure by a factor ranging from 1.5 to 12.3 times compared to conventional computed tomography (CT) scans, thus enhancing patient safety while preserving imaging accuracy [13,14]. Moreover, CBCT is cost-effective and widely available, rendering it a pragmatic option for investigating the intricate variations of the PSAA [15] [16]. Studies utilizing conventional CT scans report a lower prevalence rate of the PSAA, raising pertinent questions about its suitability for visualizing the PSAA. Therefore, CBCT has emerged as a compelling and reliable imaging modality [15].

Although numerous studies have investigated anatomical variations of the PSAA, most have focused on populations from Asia, Europe, and North America. These studies consistently report differences in the artery's location relative to the sinus wall, its calibre, and distances to various landmarks, often influenced by factors such as ethnicity, gender, and side. However, a significant gap remains in the literature regarding its characteristics from a predominantly African population, which may vary considerably in light of previous research on the subject [11] [12] [17]-[19]. To the best of the authors' knowledge, this is one of the first studies to investigate the PSAA in a Sub-Saharan setting. Thus, this study aims to provide a comprehensive assessment of the PSAA, focusing on key variables such as its diameter, relationship to the lateral sinus wall, distance to the sinus floor, and alveolar crest, all of which are crucial considerations during SFE. Such insights are crucial for enhancing the safety and predictability of SFE, thereby minimizing the risk of intraoperative complications and improving patient safety.

2. Materials and Methods

This radiological study was approved by the Kenyatta National Hospital—University of Nairobi Ethics and Research Committee (KNH-UON ERC), protocol number P814/10/2023. To address the objectives of this research, we conducted a retrospective cross-sectional study. A waiver for informed consent was approved, as the scans used in the study were collected retrospectively. The study population consisted of CBCT scans from dentate adult patients who were referred to Digital Healthcare Solutions in Nairobi, Kenya, for pretreatment scanning related to dental implants, maxillofacial surgery, orthodontics, endodontics, and oral pathology. The inclusion criteria of the sample were: 1) Left and right CBCT scan of the full maxilla; 2) Absence of any notable pathology, growth disorder or defect involving the maxillary sinus, alveolar process of the maxilla and maxillary teeth; 3) good quality CBCT free from distortion, artefacts, or foreign bodies; 4) Permanent dentition; 5) Presence of all teeth from central incisors to the second molar. Any scans that did not meet these criteria were excluded from the study. The final sample group included data from 178 CBCT scans—95 males and 83 females.

The equipment used to acquire CBCT scans was an Orthophos SL digital imag-

ing system. The images were obtained at 90 kV, 10 mA with a voxel size of 76.5 μm^3 and a 200 μm image resolution. All images were viewed with a 19-inch LCD monitor (HP L1910, Hewlett-Packard Development Co., Palo Alto, CA, USA) with 1280 × 1024 pixel resolution. The 3D Slicer medical imaging platform was used to analyze the scans. To standardize all measurements, the team reviewing the scans (KS and JN) was calibrated on data collection by a board-certified oral and maxillofacial radiologist. This process involved a thorough joint review of 32 (18%) representative CBCT scans using the 3D Slicer medical imaging platform, and an agreement was reached on anatomical reference points, including the lateral sinus wall, alveolar crest, and sinus floor. To assess inter-observer and intra-observer reliability, 35 CBCT scans (20%) were randomly selected and re-evaluated after a two-week interval. The re-evaluation was blinded to prior measurements. Intra-observer reliability yielded an intraclass correlation coefficient (ICC) of 0.91, while inter-observer reliability achieved an intraclass correlation coefficient (ICC) of 0.88, indicating excellent consistency. No statistically significant differences were found between repeated measurements ($p = 0.832$), confirming measurement reproducibility.

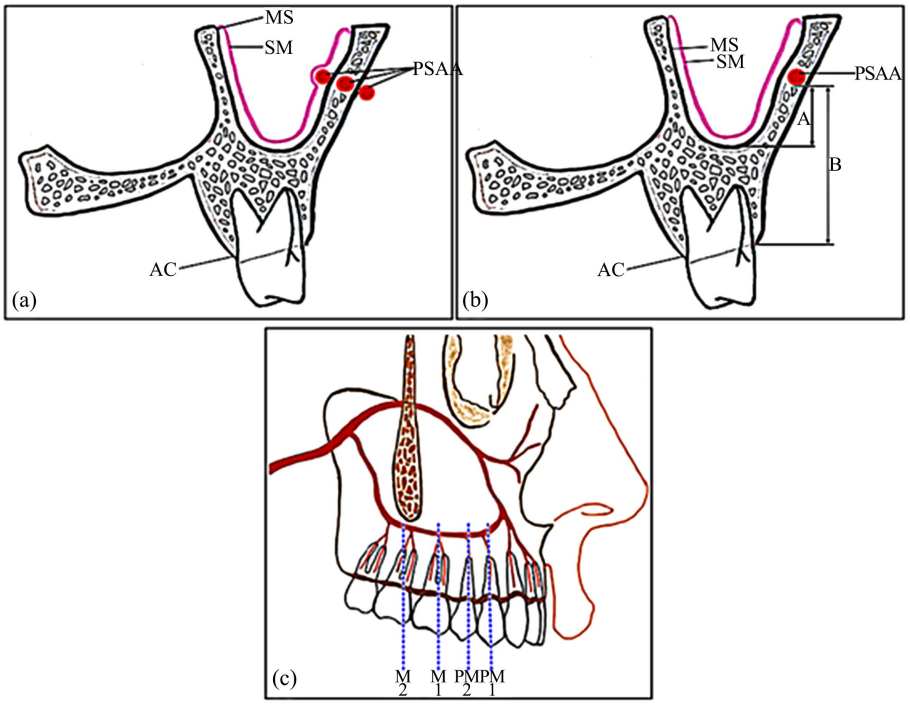

Figure 1. (a)—Coronal illustration of the maxilla showing the possible variations of the PSAA either located beneath the sinus membrane, intraosseously in the lateral wall of the sinus, or on the external cortex of the lateral wall. MS—Maxillary sinus, SM—Schneiderian membrane, AC—Alveolar crest. (b)—Coronal illustration of the maxilla showing the measurements performed. A—Distance from the PSAA to the floor of the Maxillary sinus. (c)—Lateral illustration of the maxilla showing the location in the coronal plane where measurements were made. PM1—1st premolar, PM2—2nd premolar, M1—1st molar, M2—2nd molar. *(Adapted from Yang et al. with permission under the Creative Commons Attribution* 4.0 *International License*) [20].

The independent variables were gender and side. Gender was classified as either male or female, and side was designated as either right or left. The dependent variables were the rate of detection of the PSAA (presence or absence of the PSAA), the vessel's diameter, its location relative to the lateral wall of the maxillary sinus (classified as either intraosseous, beneath the sinus membrane to or on the external cortex), the distance of the PSAA from the floor of the maxillary sinus (measured from the most inferior point of the sinus floor to the inferior border of the PSAA), and the distance of the PSAA from the alveolar crest (measured from the mid-point the buccal plate to the inferior border of the PSAA). These observations and measurements were made at 4 points: region of the first premolar (PM1), second premolar (PM2), first molar (M1), and second molar (M2) (**Figure 1**). In the event accessory branches of the PSAA were encountered, the additional branch underwent similar scrutiny.

Statistical analysis was performed using SPSS software (IBM Version 29.0; Armonk, NY). Descriptive statistics were computed and organized in tables. The confidence intervals (CI) and standard error of the mean (SEM) were calculated for each measurement. To scrutinize any variations of the PSAA, analysis was conducted to reveal any gender disparities and side differences. The chi-square test was employed for all categorical variables, while the independent t-test was employed for all continuous variables. A threshold of $P < 0.05$ was considered statistically significant. This manuscript adheres to the Strengthening the Reporting of Observational Studies in Epidemiology (STROBE) guidelines.

3. Results

3.1. Sample Characteristics and Rate of Detection of the PSAA

A total of 487 CBCT scans were initially retrieved. Of these, 275 were excluded during the initial screening due to either incomplete imaging or the absence of the region of interest. An additional 34 scans were excluded for not meeting the inclusion criteria. Ultimately,178 CBCT scans were included in the analysis, comprising 95 males and 83 females (**Figure 2**). The average age of participants was 31.4 ± 5.9 years, ranging from 21 to 37 years. The PSAA was identified bilaterally in 150 scans (84.3%), belonging to 82 males and 68 females. Unilateral PSAA was detected in 2 cases on the right side, both of which were males (1.12%). In 26 scans (14.6%), the PSAA was undetected: 11 males and 15 females. There was no statistically significant difference in the prevalence of the PSAA between males and females (Chi-square; $P = 0.551$). Owing to the low detection of unilateral PSAAs, subsequent analysis was performed on only the bilateral cases.

3.2. Diameter of the PSAA

The adjusted mean diameter of the PSAA was 1.67 ± 0.34 mm (SEM ± 0.020 mm; 95% CI: 1.64 - 1.72 mm), ranging from 1.04 mm to 2.14 mm. When assessed based on side, the mean diameter on the right side was 1.64 ± 0.31 mm (SEM ± 0.025 mm; 95% CI: 1.59 - 1.69 mm), while on the left mean diameter was 1.67 ± 0.40

mm (SEM ± 0.033 mm; 95% CI: 1.61 - 1.73 mm). There were no statistically significant differences between the left and right sides. Regarding gender dimorphism, the males had a higher average at 1.81 ± 0.30 mm (SEM ± 0.033 mm; 95% CI: 1.75 - 1.87 mm) compared to females at 1.52 ± 0.34 mm (SEM ± 0.041 mm; 95% CI: 1.44 - 1.60 mm). However, this difference was not statistically significant. The largest values were observed in the M2 region, while the PM1 region exhibited the smallest diameters across both genders. Statistical analysis revealed significant differences between the left and right sides in diameter at several positions, particularly at M2, M1, and PM2 (P-value < 0.05) (Table 1).

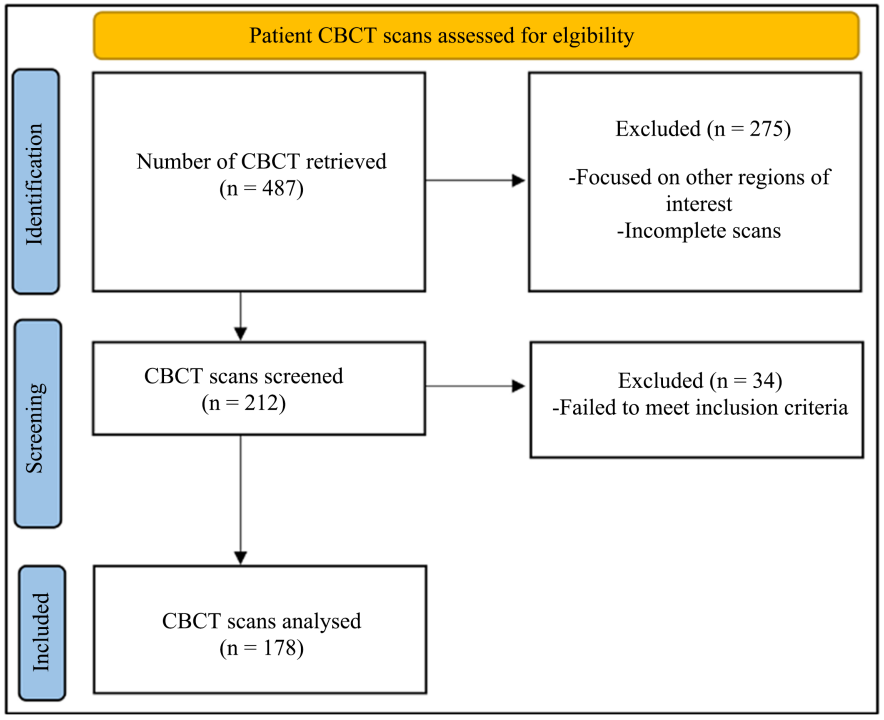

Figure 2. STROBE flowchart showing the CBCT screening for the study (STROBE: Strengthening the Reporting of Observational Studies in Epidemiology).

Table 1. Diameter of the PSAA at the various anatomical positions by side and gender, with the student t-tests for statistical comparison. *Represents statistically significant P-values.

SIDE POSITION & GENDER		RIGHT ± SD (mm)	LEFT ± SD (mm)	*MEAN* ± SD (mm)	P-value
M2	**Male**	2.14 ± 0.25	2.13 ± 0.25	2.14 ± 0.25	**0.018***
	Female	1.82 ± 0.35	2.08 ± 0.35	1.95 ± 0.35	**0.032***
M1	**Male**	1.99 ± 0.45	2.01 ± 0.45	2.00 ± 0.45	**0.040***
	Female	1.65 ± 0.55	1.61 ± 0.55	1.63 ± 0.55	0.056
PM2	**Male**	1.64 ± 0.65	1.74 ± 0.65	1.69 ± 0.65	**0.038***
	Female	1.45 ± 0.75	1.04 ± 0.75	1.25 ± 0.75	**0.049***
PM1	**Male**	1.34 ± 0.85	1.51 ± 0.85	1.42 ± 0.85	0.122
	Female	1.28 ± 0.95	1.23 ± 0.95	1.25 ± 0.95	0.135

3.3. Location of PSAA Relative to the Lateral Wall of the Maxillary Sinus

The relationship of the PSAA to the lateral wall of the maxillary sinus was found to vary across the different tooth positions (Figure 3). In the M2 region, the artery was primarily located intraosseously (48.3%), followed by the PSAA beneath the sinus membrane (32.7%), and the least on the external cortex of the lateral sinus wall (19%). A similar trend was observed in the M1 region, with the intraosseous location being the most common (65.3%). In comparison, the proportions of PSAA beneath the sinus membrane and on the external cortex were lower than that of the M2 region (14% and 20.7%, respectively). In the PM2 region, the artery was more evenly distributed between the intraosseous (45.7%) and beneath the sinus membrane locations (43.0%), with the external cortex (11.3%) location being the least frequent. In the PM1 region, the trend was comparable to PM2, with a nearly equal distribution between intraosseous (47.0%) and beneath the sinus membrane (44.7%) positions, while the external cortex location remained the least common (8.3%). Statistical analysis showed a significant difference in the distribution of the PSAA across the assessed tooth positions (Chi-square; P =< 0.001) (Table 2). A binomial analysis revealed no statistically significant differences in the position of the PSAA across genders.

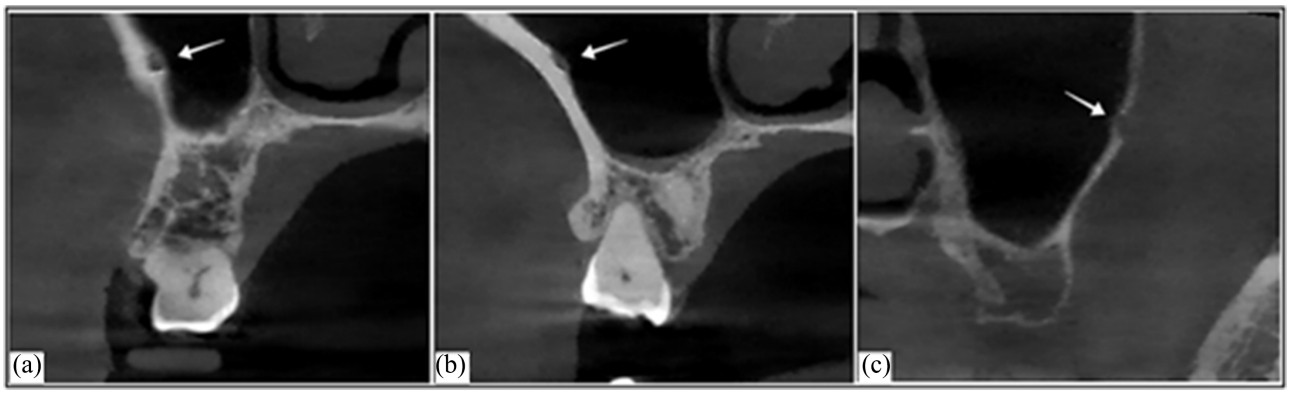

Figure 3. Relationship of the PSAA (arrows) to the lateral wall of the maxillary sinus: (a) Intraosseous, (b) beneath the sinus membrane, (c) on the external cortex.

Table 2. Distribution of the PSAA across the various tooth positions, with chi-square test for statistical comparison. * Represents statistically significant P-values.

Location	Intraosseous (%)	Beneath the Sinus Membrane (%)	On the External Cortex of the Lateral Sinus Wall (%)	P-value
M2	145 (48.3%)	57 (19.0%)	98 (32.7%)	**<0.001***
M1	196 (65.3%)	42 (14.0%)	62 (20.7%)	
PM2	137 (45.7%)	129 (43.0%)	34 (11.3%)	
PM1	141 (47.0%)	134 (44.7%)	25 (8.3%)	

3.4. Distance of PSAA to the Floor of the Maxillary Sinus

The average distance of PSAA to the maxillary sinus floor was 13.46 ± 4.24 mm (SEM ± 0.245 mm; 95% CI: 12.98 - 13.94 mm), spanning from 3.08 mm to 19.74 mm. When assessed based on side, the mean distance on the right was 13.19 ± 2.63 mm (SEM ± 0.215 mm; 95% CI: 12.77 - 13.61 mm), while on the left, it was 13.72 ± 2.87 mm (SEM ± 0.234 mm; 95% CI: 13.26 - 14.18 mm). There was no statistically significant difference between these values. Regarding gender dimorphism, the males had a higher average at 13.70 ± 2.92mm (SEM ± 0.322 mm; 95% CI: 13.07 - 14.33 mm) than females at 13.22 ± 2.58 mm (SEM ± 0.313 mm; 95% CI: 12.61 - 13.83 mm). However, this difference was also not statistically significant. The results show that the greatest distance from the sinus floor was at the M2 position. The distance generally decreased at M1 and PM2 and increased as PM1 was approached. The most significant variability between the males and females was seen at M2 and PM1, with a statistically significant difference between the right and left sides (Table 3).

Table 3. Distance of the PSAA to the maxillary sinus floor at the various anatomical positions by side and gender, with the student t-tests for statistical comparison. * Represents statistically significant P-values.

SIDE POSITION & GENDER		RIGHT ± SD (mm)	LEFT ± SD (mm)	*MEAN* ± SD (mm)	P-value
M2	**Male**	13.86 ± 3.44	15.18 ± 3.29	14.52 ± 3.37	**0.001***
	Female	13.97 ± 2.49	12.85 ± 3.84	13.41 ± 3.24	0.054
M1	**Male**	13.32 ± 3.61	13.49 ± 4.68	13.41 ± 4.18	0.964
	Female	12.70 ± 2.70	13.25 ± 3.71	12.97 ± 3.24	0.889
PM2	**Male**	12.08 ± 4.83	13.83 ± 3.59	12.96 ± 4.26	0.526
	Female	12.85 ± 2.17	12.55 ± 3.78	12.70 ± 3.08	0.137
PM1	**Male**	13.27 ± 4.64	14.53 ± 3.41	13.90 ± 4.07	0.192
	Female	13.47 ± 3.55	14.10 ± 3.27	13.79 ± 3.41	**0.018***

3.5. Distance of PSAA to the Alveolar Crest

The average distance from the PSAA to the alveolar crest was 22.53 ± 2.32 mm (SEM ± 0.134 mm; 95% CI: 22.27 - 22.79 mm), with a range spanning from 14.25 mm to 24.19 mm. When assessed based on side, the mean distance on the right was 22.04 ± 2.09 mm (SEM ± 0.171 mm; 95% CI: 21.71 - 22.37 mm), while on the left, it was 22.32 ± 2.26 mm (SEM ± 0.185 mm; 95% CI: 21.96 - 22.68 mm). There was no statistically significant difference between the right and left sides. In terms of gender dimorphism, the males had a higher average at 22.67 ± 2.51 mm (SEM ± 0.277 mm; 95% CI: 22.13 - 23.21 mm) compared to females, which was 22.39 ± 2.12 mm (SEM ± 0.257 mm; 95% CI: 21.89 - 22.89 mm). However, this difference was not statistically significant. The results show that the greatest distance from the alveolar crest was at the M2 position, with a progressive decrease at M1 and

PM2, followed by a slight increase at PM1. There was no statistically significant difference between the right and left sides across most positions, except for M1 (Table 4).

Table 4. Distance of the PSAA to the alveolar crest at the various anatomical positions by side and gender, with the student t-tests for statistical comparison. *Represents statistically significant P-values.

SIDE POSITION & GENDER		RIGHT ± SD (mm)	LEFT ± SD (mm)	*MEAN* ± SD (mm)	P-value
M2	Male	24.19 ± 1.57	23.86 ± 1.33	24.03 ± 1.76	0.224
	Female	23.12 ± 2.93	23.40 ± 2.63	23.24 ± 2.78	0.741
M1	Male	22.06 ± 2.16	22.49 ± 2.47	22.23 ± 2.39	0.087
	Female	20.53 ± 2.02	20.69 ± 1.76	20.54 ± 1.91	0.378
PM2	Male	20.35 ± 2.75	20.07 ± 3.11	20.34 ± 2.82	0.118
	Female	18.91 ± 2.46	18.99 ± 2.04	19.01 ± 2.46	0.455
PM1	Male	22.39 ± 1.73	22.52 ± 1.44	22.38 ± 1.73	0.276
	Female	22.49 ± 1.59	22.01 ± 1.11	22.52 ± 1.66	**0.003***

3.6. Accessory Branches of the PSAA

In 27.34% (n = 82) of maxillary sinus walls, two branches of the PSAA were identified. The larger branch was analyzed along with the single PSAA cases, while the smaller branch was analyzed as an accessory branch. The accessory branch was more commonly positioned below the larger branch, but in a few instances (n = 5), it was located above it. On average, the accessory branch was located at a mean distance of 12.34 ± 3.65 mm (SEM ± 0.403 mm; 95% CI: 11.55 - 13.13 mm) from the maxillary sinus floor and 21.89 ± 3.51 mm from the alveolar crest (SEM ± 0.388 mm; 95% CI: 21.13 - 22.65 mm). The average distance between the two branches was 3.23 ± 1.51 mm (SEM ± 0.167 mm; 95% CI: 2.90 - 3.56 mm).

4. Discussion

Lateral SFE is frequently carried out in cases where the vertical height of the residual alveolar ridge is less than 4mm to facilitate Schneiderian membrane detachment and lifting from the maxillary sinus floor, followed by grafting [3]. However, given that the Schneiderian membrane has an average thickness of just 1.17 ± 0.1 mm, it is prone to perforation during the procedure [21]. This risk is further amplified when haemorrhage from the PSAA obscures the surgical field, making visualization and manipulation more challenging. Injury to the PSAA most often occurs when rotary instruments are used to create the lateral bony window, emphasizing the need for precise surgical technique. As a result, lateral SFE can be particularly demanding for inexperienced clinicians and even seasoned surgeons. Designing an optimal lateral window is one of the most critical steps in ensuring a smooth procedure. It must be large enough to provide adequate visibility, allow for safe Schneiderian membrane elevation, and facilitate the proper placement of bone

graft material. Achieving this requires a comprehensive preoperative analysis of the maxillary sinus, considering potential anatomical variations of the PSAA [22], which may be influenced by population-specific differences in craniofacial morphology and sinus pneumatization patterns that are known to vary among various groups.

4.1. Rate of Detection of the PSAA

In the present study, the PSAA was detected in 84.3% of cases—a rate similar to that reported in Turkish (80.6% and 89.3%) and Iranian (87.0%) populations [11] [18]. In contrast, detection rates in other populations have been higher among Malays (91.6%), Iranians (93.0%), and Thais (94.6%), and lower among Japanese (74.5%), Iranians (71.0%), Indians (70.0%), Americans (64.5% and 52.9%), Israelis (55.0%), and French (10.5%) [9] [10] [12] [13] [15] [19] [23]-[26]. Studies using CT scans report lower detection rates than those employing CBCT. This is likely because CT, with a spatial resolution of 0.5 to 0.8 mm, may miss finer canals, meaning that an undetected PSAA on CT does not confirm its absence [26]. In contrast, cadaveric studies report a 100% detection rate, suggesting that radiological imaging may underestimate the true prevalence of the PSAA [27]-[29]. These discrepancies in radiological detection rates likely stem from differences in imaging equipment, techniques, CBCT data interpretation, and the inherent challenges of visualizing small-calibre vessels.

4.2. Diameter of the PSAA

In the present study, the mean diameter of the PSAA was 1.67 ± 0.34 mm, which is higher than that reported in the existing literature [10] [15] [16] [30] [31]. Larger arteries pose a more significant potential for significant hemorrhagic episodes. Apostolakis et al. highlighted that vessels with a diameter greater than 2 mm could lead to excessive bleeding but non-life-threatening complications [32]-[34]. Our findings indicate that the largest diameters of the PSAA are found in the M2 and M1 regions, where the average diameter exceeds the 2mm threshold. This emphasizes the importance of vigilance on the surgeon's part, as extending the lateral window approach too far posteriorly may increase the likelihood of more severe haemorrhage.

4.3. Location of PSAA Relative to the Lateral Wall of the Maxillary Sinus

A large proportion of existing studies evaluate the relationship of the PSAA to the lateral wall of the maxillary sinus at a single location and generalize those findings for the entire course of the vessel [10] [12] [18]. In contrast, the present results demonstrate that this relationship is dynamic and changes along the PSAA's path. Specifically, although most vessels were intraosseous in the region of M2 (48.3%), a considerable proportion (32.7%) was observed on the external cortex. More anteriorly, in the M1 region, the intraosseous position was observed to have increased

(65.3%), while the proportion on the external cortex decreased (20.7%), indicating that some vessels had traversed the bone to adopt an intraosseous course. Further anteriorly, in the PM2 and PM1 regions, the PSAA was almost equally distributed between intraosseous and beneath the sinus membrane, suggesting an additional shift as the vessel pierced the medial aspect of the lateral wall to now enter the maxillary sinus. Nevertheless, compared with the systematic review and meta-analysis by Radmand *et al*., the findings of this study are concordant in demonstrating that the most frequent location of the PSAA is intraosseous, with no significant influence of gender on arterial positioning [17].

There is a scarcity of data concerning the investigation of dynamic changes in the relationship between the PSAA and the lateral wall of the maxillary sinus at different locations among the African population groups. However, this information is highly significant when utilizing a lateral window approach to the sinus. Variations in the PSAA's positioning can elevate the risk of bleeding and hinder the healing process. This variability is essential for accurate preoperative planning, which includes thorough radiographic assessments to identify and safeguard the PSAA. Understanding how the artery might penetrate or navigate through the bony wall is vital for refining surgical techniques, thereby reducing the risk of haemorrhage and other potential complications.

4.4. Distance of PSAA to the Floor of the Maxillary Sinus

The average distance from the PSAA to the maxillary sinus floor in the present study was 13.46 ± 4.24 mm, falling within the range reported for Thai and Malay populations [9] [24], but exceeding the mean of 8.85 ± 0.4 mm described for Egyptian, Korean, Iranian, Chinese, and Turkish groups [8] [16] [35]-[40]. Such differences may be due to geographic and genetic factors. Notably, because the artery in our sample is positioned slightly higher than the international mean, surgeons may have somewhat more leeway when planning the location of the lateral window during SFE. This study also reveals a previously undescribed trend: the distance from the PSAA is greatest in the M2 region, descends toward M1 (reaching its lowest point near PM2), and ascends again in the PM1 region. From a clinical standpoint, this indicates that the surgeon must exercise caution around the area of the second premolar and the first molar, as the PSAA is located at a more inferior compared to the first premolar and second molar regions.

Overall, no statistically significant sex-based differences were found, consistent with results in Malays, Indians, Koreans, and Tehranis [9] [15] [41] [42], although greater distances have been reported in males among Thai and Turkish populations [24] [38].

4.5. Distance of PSAA to the Alveolar Crest

The distance of the PSAA to the alveolar crest was found to be 22.53 ± 2.32 mm in the present study. This is higher than the means reported among the Iranian, Turkish, Korean, Columbian, Spanish, and Indian groups [8] [10] [11] [30] [31]

[35] [39] [43]-[45]. Based on existing literature, a distance of 15mm superior to the alveolar crest is considered safe for placement of the osteotomy in the lateral window approach to the maxillary sinus [17]. Our study corroborates these findings as the average reported in this study is more than adequate. These findings may influence not only sinus augmentation procedures but also the selection of implant length in the posterior maxilla. Of note is that in the M1 and PM2 regions, the vessel descends slightly inferiorly than in the M2 and PM1 regions, a finding that has not yet been explored further in the literature. The distance between the alveolar crest and the PSAA is not significantly affected in partially edentulous patients and may be comparable to dentate patients. The existing literature indicates that it changes significantly only in fully edentulous cases [17].

4.6. Accessory Branches of the PSAA

Two branches of the PSAA were found in 27.34% of cases in this study. This is lower than that described in the Malays but higher than the Egyptian population groups [9] [16]. The importance of this finding is that when performing elective surgeries, such as the Caldwell-Luc operation, Le Fort I osteotomy, and SFE, the position of these branches should be known to avoid bleeding that may obscure the surgical field and lengthen procedure times [9].

4.7. Clinical Surgical Implications

Taken together, the anatomical patterns demonstrated in this study highlight that the PSAA follows a regionally variable and surgically consequential trajectory, which must be accounted for in lateral sinus floor elevation. The artery does not maintain a uniform position; rather, its course shifts progressively along the posterior maxilla, altering its depth and proximity to key surgical landmarks. The increase in vessel diameter in the molar region, combined with its closer relationship to both the sinus floor and alveolar crest around the first molar and second premolar, designates this zone as the highest-risk corridor for intraoperative hemorrhage. Furthermore, the transition from an external cortical or intraosseous course posteriorly to a sub-membranous path anteriorly means that the artery may be encountered at different layers of dissection, requiring the surgeon to adjust both window height and depth of bone removal dynamically rather than adhering to a standardized profile. These multidimensional variations mean that the lateral window design must be site-specific, guided by the actual vascular topography revealed radiographically, rather than derived from generalized textbook distances. Therefore, high-resolution CBCT evaluation is not merely recommended but clinically indispensable, serving as the basis for tailoring the osteotomy, minimizing Schneiderian membrane perforation, and reducing arterial injury risk.

4.8. Avoiding Damage to the PSAA Intraoperatively

Maintaining a low window antrostomy design with a mesiodistal extent of 15-20mm is advisable [4] [46]. A window height of 6-8mm at most prevents damage

to most intraosseous vessels. Anteriorly, the osteotomy line should be placed flush with the anterior wall of the sinus to eliminate blind spots caused by the mesial recess. Inferiorly, the lower horizontal line should also be flush with the sinus floor to remove any residual bone wall that might obstruct the detachment of the sinus membrane. Distally, the osteotomy window should correspond to the location of the most posteriorly planned implant. From the current study, we recommend that the superior horizontal line should not be perfectly straight. Instead, it should have a slight inferior (coronal) curve around the area of the second premolar and first molar when compared to the first premolar and second molar regions. This adjustment will help prevent injury to the PSAA, which is generally located closer to the sinus floor and alveolar crest in these specific areas.

Computer-guided antrostomy using surgical stents designed in dedicated softwares has been advocated to improve the surgical accuracy of SFE [47]. Although promising, this technique has not been systematically evaluated in large-scale clinical studies; the current evidence supporting its application remains largely anecdotal. Consequently, it remains imperative for the clinician to possess a sound understanding of maxillary sinus anatomy, particularly variations in the PSAA course and location, to accurately interpret CBCT data and plan the antrostomy even when using digital guides.

A thorough understanding of anatomical variations, such as the presence of multiple arterial branches, an external cortical course of the artery, or the proximity of a sinus septum to the osteotomy site, is also critical. To enhance safety and control, it is advisable first to thin the lateral sinus wall using ultrasonic instrumentation before fully opening the window. This staged approach facilitates early identification of the PSAA as it courses either intraosseously or beneath the Schneiderian membrane, enabling the surgeon to adjust the antrostomy design and avoid vessel injury [48].

The use of piezoelectric surgical devices allows for precise bone cutting while preserving adjacent soft tissue structures, including the PSAA [49]. Several studies have reported that piezoelectric systems, compared to conventional rotary instruments, are associated with significantly fewer intraoperative complications [48] [49].

Preoperative CBCT evaluation should, therefore, be mandatory to identify high-risk vascular structures and adapt the antrostomy design accordingly, reducing the risk of intraoperative bleeding and membrane perforation.

4.9. How to Manage Intraoperative Bleeding from the PSAA

In cases of significant intraoperative bleeding, it is recommended to apply direct pressure using gauze initially and to utilize a localized vasoconstrictor. Should the haemorrhage continue and the affected vessel is intraosseous, alternative methods may involve the application of bone wax, compressing the bone channel surrounding the vessel with a hemostat, or employing electrocauterization [5] [50]. However, caution must be exercised with the latter as this may risk the integrity of the

sinus membrane. It is also suggested that it may be beneficial to avoid suturing the distal incision site as this may facilitate the expulsion of any clots [51].

5. Strengths and Limitations

The strength of the present study is in its rigorous methodology, which involved evaluating multiple parameters of the PSAA in an underrepresented population. Nevertheless, the study had a limitation the sample consisted exclusively of patients who were fully dentate in the posterior maxilla. As such, the measurements relating distance from the alveolar crest are specific to dentate individuals and may not be directly generalizable to edentulous cases, where alveolar bone resorption alters crest height and morphology. Additionally, this study consisted of a relatively small sample size of 178 CBCT scans, which may limit its generalizability and may not apply to patients exhibiting the less common unilateral vascular anatomy. Although this falls within the range of other studies that focus on the PSAA, further studies would be necessary to corroborate these findings in this population group. Furthermore, the CBCT imaging system used had an inherent slice thickness of 0.3 mm, which could be considered a limitation in detecting smaller-diameter PSAA. Future research studies with a larger sample size could provide data that is much more generalizable.

6. Conclusion

Preoperative radiological evaluation of the maxillary sinus using CBCT scanning is essential for identifying the presence, location, variations, and dimensions of the PSAA. In the second molar region, the PSAA is found extraosseous and then follows an intraosseous pathway in the first molar area, eventually assuming a medial position of the lateral maxillary wall, specifically in the premolar region. The PSAA is found 13.46 mm superior to the maxillary sinus floor and 22.53 mm superior to the alveolar crest. The PSAA is in a much coronal position in the region of the second premolar and first molar. In the absence of a surgical guide, it would be recommended that the antrostomy preparation for the lateral SFE be performed as mesially and as low as possible with a slight inferior (coronal) curve around the area of the second premolar and first molar to avoid encountering PSAA or its variants.

Author Contributions

Krishan Sarna—Conceptualization, Methodology, Software, Validation, Formal analysis, Investigation, Data Curation, Writing - Original Draft, Writing - Review & Editing

Fawzia Butt—Conceptualization, Methodology, Resources, Writing - Original Draft, Writing - Review & Editing, Supervision, Project administration

Joseph Gakonyo—Conceptualization, Methodology, Resources, Writing - Original Draft, Writing - Review & Editing, Supervision, Project administration

Jimmy Gakure Njoroge—Methodology, Data Curation, Software, Validation,

Writing - Original Draft, Writing - Review & Editing

Beda Olabu—Conceptualization, Methodology, Writing - Review & Editing, Supervision, Project administration

Conflicts of Interest

The authors declare no conflict of interest.

Funding Sources

This research received no specific grant from funding agencies in the public, commercial, or not-for-profit sectors.

Acknowledgement

The authors would like to thank all who made the completion of this manuscript possible, especially Digital Healthcare Solutions for allowing the CBCT images to be used

References

[1] Pjetursson, B.E., Tan, W.C., Zwahlen, M. and Lang, N.P. (2008) A Systematic Review of the Success of Sinus Floor Elevation and Survival of Implants Inserted in Combination with Sinus Floor Elevation: Part I: Lateral Approach. *Journal of Clinical Periodontology*, **35**, 216-240. https://doi.org/10.1111/j.1600-051x.2008.01272.x

[2] Lam, L., Ivanovski, S. and Lee, R.S.B. (2024) Alveolar Ridge Preservation in Posterior Maxillary Teeth for Reduction in the Potential Need for Sinus Floor Elevation Procedures: A Pilot Study. *Clinical Oral Implants Research*, **35**, 1568-1584. https://doi.org/10.1111/clr.14344

[3] Starch-Jensen, T. and Jensen, J.D. (2017) Maxillary Sinus Floor Augmentation: A Review of Selected Treatment Modalities. *Journal of Oral and Maxillofacial Research*, **8**, e3. https://doi.org/10.5037/jomr.2017.8303

[4] Testori, T., Rosano, G., Taschieri, S. and Del Fabbro, M. (2010) Ligation of an Unusually Large Vessel during Maxillary Sinus Floor Augmentation. A Case Report. *European journal of oral implantology*, 3, 255-258.

[5] Testori, T., Tavelli, L., Scaini, R., Saibene, A.M., Felisati, G., Barootchi, S., *et al.* (2023) How to Avoid Intraoperative and Postoperative Complications in Maxillary Sinus Elevation. *Periodontology* 2000, **92**, 299-328. https://doi.org/10.1111/prd.12480

[6] Çam, K. and Zengin, A.Z. (2025) Evaluation of the Location of Posterior Superior Alveolar Artery and Infraorbital Foramen Originating from the Same Source by Using Cone Beam Computed Tomography. *BMC Oral Health*, **25**, Article No. 105. https://doi.org/10.1186/s12903-024-05408-x

[7] Ataman-Duruel, E.T., Duruel, O., Turkyilmaz, I. and Tözüm, T.F. (2019) Anatomic Variation of Posterior Superior Alveolar Artery: Review of Literature and Case Introduction. *Journal of Oral Implantology*, **45**, 79-85. https://doi.org/10.1563/aaid-joi-d-18-00056

[8] Shams, N., Dabbaghi, A., Shams, B., Naderi, L. and Rakhshan, V. (2020) Anatomy of the Posterior Superior Alveolar Artery: A Cone-Beam Computed Tomographic Study. *Journal of Maxillofacial and Oral Surgery*, **21**, 203-210. https://doi.org/10.1007/s12663-020-01386-z

[9] Ang, K., Ang, K. and Ngeow, W.C. (2022) The Prevalence and Location of the Posterior Superior Alveolar Artery in the Maxillary Sinus Wall: A Preliminary Computed-Cone Beam Study. *The Saudi Dental Journal*, **34**, 629-635. https://doi.org/10.1016/j.sdentj.2022.08.010

[10] Chitsazi, M., Shirmohammadi, A., Faramarzi, M., Esmaieli, F. and Chitsazi, S. (2017) Evaluation of the Position of the Posterior Superior Alveolar Artery in Relation to the Maxillary Sinus Using the Cone-Beam Computed Tomography Scans. *Journal of Clinical and Experimental Dentistry*, **9**, e394-e399. https://doi.org/10.4317/jced.53213

[11] Ilguy, D., Ilguy, M., Dolekoglu, S. and Fisekcioglu, E. (2013) Evaluation of the Posterior Superior Alveolar Artery and the Maxillary Sinus with CBCT. *Brazilian Oral Research*, **27**, 431-437. https://doi.org/10.1590/s1806-83242013000500007

[12] Güncü, G.N., Yildirim, Y.D., Wang, H. and Tözüm, T.F. (2011) Location of Posterior Superior Alveolar Artery and Evaluation of Maxillary Sinus Anatomy with Computerized Tomography: A Clinical Study. *Clinical Oral Implants Research*, **22**, 1164-1167. https://doi.org/10.1111/j.1600-0501.2010.02071.x

[13] Ella, B., Sédarat, C., Noble, R.D.C., *et al.* (2008) Vascular Connections of the Lateral Wall of the Sinus: Surgical Effect in Sinus Augmentation. *The International Journal of Oral & Maxillofacial Implants*, **23**, 1047-1052.

[14] Cagici, C.A., Yilmazer, C., Hurcan, C., Ozer, C. and Ozer, F. (2008) Appropriate Interslice Gap for Screening Coronal Paranasal Sinus Tomography for Mucosal Thickening. *European Archives of Oto-Rhino-Laryngology*, **266**, 519-525. https://doi.org/10.1007/s00405-008-0786-6

[15] Pandharbale, A.A., Gadgil, R.M., Bhoosreddy, A.R., Kunte, V.R., Ahire, B.S., Shinde, M.R., *et al.* (2016) Evaluation of the Posterior Superior Alveolar Artery Using Cone Beam Computed Tomography. *Polish Journal of Radiology*, **81**, 606-610. https://doi.org/10.12659/pjr.899221

[16] Fayek, M.M., Amer, M.E. and Bakry, A.M. (2021) Evaluation of the Posterior Superior Alveolar Artery Canal by Cone-Beam Computed Tomography in a Sample of the Egyptian Population. *Imaging Science in Dentistry*, **51**, 35-40. https://doi.org/10.5624/isd.20200146

[17] Radmand, F., Razi, T., Baseri, M., Gavgani, L.F., Salehnia, F. and Faramarzi, M. (2023) Anatomic Evaluation of the Posterior Superior Alveolar Artery Using Cone-Beam Computed Tomography: A Systematic Review and Meta-Analysis. *Imaging Science in Dentistry*, **53**, 177-191. https://doi.org/10.5624/isd.20230009

[18] Yalcin, E.D. and Akyol, S. (2019) Relationship between the Posterior Superior Alveolar Artery and Maxillary Sinus Pathology: A Cone-Beam Computed Tomography Study. *Journal of Oral and Maxillofacial Surgery*, **77**, 2494-2502. https://doi.org/10.1016/j.joms.2019.07.009

[19] Tsukioka, T., Muraoka, H., Ito, K., Hirahara, N., Okada, S. and Kaneda, T. (2021) Detection of Posterior Superior Alveolar Artery Using Multi-Detector Row CT: A Retrospective Study Focused on Age-Related Changes. *Oral Radiology*, **38**, 344-348. https://doi.org/10.1007/s11282-021-00562-2

[20] Yang, D.H. and Lee, N.V. (2021) A Simple Method of Managing the Alveolar Antral Artery during Sinus Lift Surgery. *International Journal of Otolaryngology and Head & Neck Surgery*, **10**, 131-146. https://doi.org/10.4236/ijohns.2021.103014

[21] Monje, A., Diaz, K.T., Aranda, L., Insua, A., Garcia-Nogales, A. and Wang, H. (2016) Schneiderian Membrane Thickness and Clinical Implications for Sinus Augmentation: A Systematic Review and Meta-Regression Analyses. *Journal of Periodontology*,

87, 888-899. https://doi.org/10.1902/jop.2016.160041

[22] Gulec, M., Icen, V. and Ozmen, E.E. (2025) Evaluation of Maxillary Sinus Pathologies and the Posterior Superior Alveolar Artery Canal Using Cone-Beam Computed Tomography. *BMC Oral Health*, **25**, Article No. 70. https://doi.org/10.1186/s12903-025-05452-1

[23] Shahidi, S., Zamiri, B., Momeni Danaei, S., Salehi, S. and Hamedani, S. (2016) Evaluation of Anatomic Variations in Maxillary Sinus with the Aid of Cone Beam Computed Tomography (CBCT) in a Population in South of Iran. *Journal of Dentistry*, **17**, 7-15.

[24] Laovoravit, V., Kretapirom, K. and Pornprasertsuk-Damrongsri, S. (2020) Prevalence and Morphometric Analysis of the Alveolar Antral Artery in a Group of Thai Population by Cone Beam Computed Tomography. *Oral Radiology*, **37**, 452-462. https://doi.org/10.1007/s11282-020-00478-3

[25] Elian, N., Wallace, S., Cho, S.C., Jalbout, Z.N. and Froum, S. (2005) Distribution of the Maxillary Artery as It Relates to Sinus Floor Augmentation. *The International Journal of Oral & Maxillofacial Implants*, **20**, 784-787.

[26] Mardinger, O., Abba, M., Hirshberg, A. and Schwartz-Arad, D. (2007) Prevalence, Diameter and Course of the Maxillary Intraosseous Vascular Canal with Relation to Sinus Augmentation Procedure: A Radiographic Study. *International Journal of Oral and Maxillofacial Surgery*, **36**, 735-738. https://doi.org/10.1016/j.ijom.2007.05.005

[27] Solar, P., Geyerhofer, U., Traxler, H., Windisch, A., Ulm, C. and Watzek, G. (1999) Blood Supply to the Maxillary Sinus Relevant to Sinus Floor Elevation Procedures. *Clinical Oral Implants Research*, **10**, 34-44. https://doi.org/10.1034/j.1600-0501.1999.100105.x

[28] Traxler, H., Windisch, A., Geyerhofer, U., Surd, R., Solar, P. and Firbas, W. (1999) Arterial Blood Supply of the Maxillary Sinus. *Clinical Anatomy*, **12**, 417-421. https://doi.org/10.1002/(sici)1098-2353(1999)12:6<417::aid-ca3>3.0.co;2-w

[29] Rosano, G., Taschieri, S., Gaudy, J., Weinstein, T. and Del Fabbro, M. (2010) Maxillary Sinus Vascular Anatomy and Its Relation to Sinus Lift Surgery. *Clinical Oral Implants Research*, **22**, 711-715. https://doi.org/10.1111/j.1600-0501.2010.02045.x

[30] Kawakami, S., Botticelli, D., Nakajima, Y., Sakuma, S. and Baba, S. (2019) Anatomical Analyses for Maxillary Sinus Floor Augmentation with a Lateral Approach: A Cone Beam Computed Tomography Study. *Annals of Anatomy—Anatomischer Anzeiger*, **226**, 29-34. https://doi.org/10.1016/j.aanat.2019.07.003

[31] Yu, S., Lee, Y., Lin, C. and Wu, A.Y. (2019) Computed Tomographic Analysis of Maxillary Sinus Anatomy Relevant to Sinus Lift Procedures in Edentulous Ridges. *Journal of Periodontal & Implant Science*, **49**, 237-247. https://doi.org/10.5051/jpis.2019.49.4.237

[32] Apostolakis, D. and Bissoon, A.K. (2013) Radiographic Evaluation of the Superior Alveolar Canal: Measurements of Its Diameter and of Its Position in Relation to the Maxillary Sinus Floor: A Cone Beam Computerized Tomography Study. *Clinical Oral Implants Research*, **25**, 553-559. https://doi.org/10.1111/clr.12119

[33] Vercellotti, T., De Paoli, S. and Nevins, M. (2001) The Piezoelectric Bony Window Osteotomy and Sinus Membrane Elevation: Introduction of a New Technique for Simplification of the Sinus Augmentation Procedure. *International Journal of Periodontics & Restorative Dentistry*, **21**, 561-567.

[34] Stacchi, C., Troiano, G., Berton, F., *et al.* (2020) Piezoelectric Bone Surgery for Lateral Sinus Floor Elevation Compared with Conventional Rotary Instruments: A Systematic Review, Meta-Analysis and Trial Sequential Analysis. *International Journal of*

Oral Implantology, **13**, 109-121.

[35] Jung, J., Yim, J.H., Kwon, Y.D., *et al.* (2011) A Radiographic Study of the Position and Prevalence of the Maxillary Arterial Endosseous Anastomosis Using Cone Beam Computed Tomography. *The International Journal of Oral & Maxillofacial Implants*, **26**, 1273-1278.

[36] Kim, J.H., Kim, H.J., Jo, Y.J., Choi, J.S. and Moon, S.Y. (2021) 3D Volumetric Analysis and Anatomical Considerations for Sinus Bone Graft. *Applied Sciences*, **11**, Article 951. https://doi.org/10.3390/app11030951

[37] Sun, W., Liu, A., Gong, Y., Shu, R. and Xie, Y. (2018) Evaluation of the Anastomosis Canal in Lateral Maxillary Sinus Wall with Cone Beam Computerized Tomography: A Clinical Study. *Journal of Oral Implantology*, **44**, 5-13. https://doi.org/10.1563/aaid-joi-d-17-00129

[38] Karslioglu, H., Çitir, M., Gunduz, K. and Kasap, P. (2021) The Radiological Evaluation of Posterior Superior Alveolar Artery by Using CBCT. *Current Medical Imaging Formerly Current Medical Imaging Reviews*, **17**, 384-389. https://doi.org/10.2174/1573405616666200628134308

[39] Kang, S., Shin, S., Herr, Y., Kwon, Y., Kim, G. and Chung, J. (2011) Anatomical Structures in the Maxillary Sinus Related to Lateral Sinus Elevation: A Cone Beam Computed Tomographic Analysis. *Clinical Oral Implants Research*, **24**, 75-81. https://doi.org/10.1111/j.1600-0501.2011.02378.x

[40] Tassoker, M. (2022) Cone Beam CT Evaluation of Maxillary Sinus and Posterior Superior Alveolar Artery. *Selcuk Dental Journal*, **9**, 191-199. https://doi.org/10.15311/selcukdentj.846996

[41] Yang, S. and Kye, S. (2014) Location of Maxillary Intraosseous Vascular Anastomosis Based on the Tooth Position and Height of the Residual Alveolar Bone: Computed Tomographic Analysis. *Journal of Periodontal & Implant Science*, **44**, 50-56. https://doi.org/10.5051/jpis.2014.44.2.50

[42] Tran, T.B., Estrin, N.E., Saleh, M.H.A., Yoon, T.Y.H., Tattan, M. and Wang, H. (2020) Evaluation of Length and Location of the Maxillary Sinus Intraosseous Artery Using Computerized Tomography. *Journal of Periodontology*, **92**, 854-862. https://doi.org/10.1002/jper.20-0560

[43] Tehranchi, M., Taleghani, F., Shahab, S. and Nouri, A. (2017) Prevalence and Location of the Posterior Superior Alveolar Artery Using Cone-Beam Computed Tomography. *Imaging Science in Dentistry*, **47**, 39-44. https://doi.org/10.5624/isd.2017.47.1.39

[44] Velasco-Torres, M., Padial-Molina, M., Alarcón, J.A., O'Valle, F., Catena, A. and Galindo-Moreno, P. (2016) Maxillary Sinus Dimensions with Respect to the Posterior Superior Alveolar Artery Decrease with Tooth Loss. *Implant Dentistry*, **25**, 464-470. https://doi.org/10.1097/id.0000000000000445

[45] Godil, A.Z., Devadiga, T.J., Supnekar, S.C., Kazi, A.I., Wadwan, S.A. and Dugal, R. (2021) Position of Posterior Superior Alveolar Artery in Relation to the Maxillary Sinus Using Cone Beam Computed Tomography in Indian Sub-Population. *Journal of Oral Medicine and Oral Surgery*, **27**, 34. https://doi.org/10.1051/mbcb/2021007

[46] Zaniol, T., Zaniol, A., Ravazzolo, S., Testori, T. and Wallace, S. (2022) Low Window Sinus Elevation Technique: Bone Gain and Postsurgical Discomfort. A Retrospective Case Series. *The International Journal of Periodontics & Restorative Dentistry*, **42**, 449-457. https://doi.org/10.11607/prd.5731

[47] Strbac, G.D., Giannis, K., Schnappauf, A., Bertl, K., Stavropoulos, A. and Ulm, C. (2020) Guided Lateral Sinus Lift Procedure Using 3-Dimensionally Printed Tem-

plates for a Safe Surgical Approach: A Proof-Of-Concept Case Report. *Journal of Oral and Maxillofacial Surgery*, **78**, 1529-1537. https://doi.org/10.1016/j.joms.2020.04.042

[48] Valentini, P. and Stacchi, C. (2024) Prevention and Management of Intra-Operative Complications in Maxillary Sinus Augmentation: A Review. *Clinical Implant Dentistry and Related Research*, **27**, e13397. https://doi.org/10.1111/cid.13397

[49] Stacchi, C., Andolsek, F., Berton, F., Perinetti, G., Navarra, C. and Di Lenarda, R. (2017) Intraoperative Complications during Sinus Floor Elevation with Lateral Approach: A Systematic Review. *The International Journal of Oral & Maxillofacial Implants*, **32**, e107-e118. https://doi.org/10.11607/jomi.4884

[50] Wallace, S.S., Tarnow, D.P., Froum, S.J., Cho, S., Zadeh, H.H., Stoupel, J., *et al.* (2012) Maxillary Sinus Elevation by Lateral Window Approach: Evolution of Technology and Technique. *Journal of Evidence Based Dental Practice*, **12**, 161-171. https://doi.org/10.1016/s1532-3382(12)70030-1

[51] Scarano, A., Lorusso, F., Arcangelo, M., D'Arcangelo, C., Celletti, R. and De Oliveira, P.S. (2018) Lateral Sinus Floor Elevation Performed with Trapezoidal and Modified Triangular Flap Designs: A Randomized Pilot Study of Post-Operative Pain Using Thermal Infrared Imaging. *International Journal of Environmental Research and Public Health*, **15**, Article 1277. https://doi.org/10.3390/ijerph15061277